

An Efficient Numerical Technique for the Solution of a Nonlinear Capillary Wave Problem

TA-JO LIU* AND R. C. ACKERBERG

*Department of Chemical Engineering, Polytechnic Institute of New York,
Brooklyn, New York 11201*

Received February 4, 1982

Buneman's block cyclic reduction method has been modified to solve a capillary wave problem which is characterized by a nonlinear boundary condition on the free surface. This technique requires an iterative solution of only the unknown boundary values along the free streamline. Once the free surface values are known, the remaining unknowns are determined directly. Comparisons of the numerical solutions with existing exact solutions demonstrate the accuracy and efficiency of this method for handling the nonlinear boundary condition. Some generalizations of the method have also been discussed.

1. INTRODUCTION

Several direct numerical techniques have been developed to solve the discretized Poisson's equation in recent years. Among these, the direct solver which utilizes the block cyclic reduction method is considered to be one of the most efficient, since it requires the least storage and operation count [1]. This method was first applied by Buneman [2] to solve Poisson's equations with Dirichlet boundary conditions on a rectangle. Generalizations have been considered which deal with (1) different boundary conditions [3], (2) irregular domains [3–5], and (3) different coordinate systems [6, 7]. An original restriction on the order of the matrices has been removed [8, 9]. In addition to Poisson's equations, this method can also be used to solve the biharmonic equation [5], separable [10], and nonseparable [11] elliptic equations and even parabolic equations [12]. Some authors have suggested faster methods by combining the block cyclic reduction technique with the fast Fourier transform (FFT) method [13, 14] and with a marching technique [15].

We observed that due to some special properties of the reduction process, this method can be modified to efficiently solve a capillary wave problem, which is characterized by a nonlinear boundary condition on the free surface. The technique developed here is superior to conventional finite-difference iterative methods in that only the unknown values on the free streamline are involved in the iteration. After convergence is achieved, the remaining unknowns are computed directly. An exact

* Present address: Research Laboratories, Eastman Kodak Company, Rochester, New York 14650.

solution of capillary waves on water of infinite depth was first derived by Crapper [16]. Kinnersley [17] later extended Crapper's approach to obtain exact solutions for capillary waves on water of finite depth. We shall compare our numerical solutions with the exact solutions obtained by Kinnersley to verify the accuracy of the method presented here. Recently, several researchers [19–22] have studied gravity-capillary waves by representing the free surfaces with various integro-differential equations, and solving the equations numerically. Bloor [19] reported on the computation of pure capillary waves on thin sheets of water using a truncated Fourier Series but no direct comparison was made with Kinnersley's solution, although a comparison was made with Crapper's solution for water of infinite depth.

In Section 2, we formulate the capillary wave problem and present the exact solutions obtained by Kinnersley [17]. The numerical procedure to solve the problem is given in Section 3. Comparisons of the numerical solutions with the exact solutions are made in Section 4. Finally, we discuss some generalizations of the method in Section 5.

2. CAPILLARY WAVE PROBLEM WITH EXACT SOLUTION

Figure 1 illustrates the fluid motion being considered: symmetric capillary waves move with phase velocity u_0 to the right on the free surfaces of an ideal fluid sheet, and surface tension is assumed to be the only restoring force. If we introduce Cartesian coordinates (\bar{x}, \bar{y}) moving with velocity u_0 to the right with \bar{x} measured to the right and \bar{y} vertically upwards from the line of symmetry, the waves will appear to be steady. Due to the symmetry of the problem, we need only consider the flow region bounded by the line of symmetry and the free surface.

The wave motion will be assumed irrotational, and we define the complex velocity potential $\bar{w} = \bar{\phi} + i\bar{\psi}$ and the complex velocity

$$\frac{d\bar{w}}{d\bar{z}} = \bar{u} - i\bar{v} = \bar{q}e^{-i\theta}, \quad \text{where } \bar{z} = \bar{x} + i\bar{y}, \tag{1}$$

and \bar{u}, \bar{v} are the velocity components in the \bar{x}, \bar{y} directions, respectively, $\bar{q} = (\bar{u}^2 + \bar{v}^2)^{1/2}$ is the speed, and θ is the deflection angle. The free boundary is a streamline which we can take to be $\bar{\psi} = 0$ without loss of generality. If we denote the

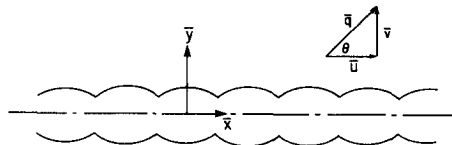


FIG. 1. Capillary waves on a thin fluid sheet.

line of symmetry (\bar{x} axis in Fig. 1) to be $\bar{\psi} = -Lu_0$, where L is one-half the thickness of the undisturbed fluid sheet, we can introduce the dimensionless variables

$$z = \bar{z}/L, \quad u = \bar{u}/u_0, \quad v = \bar{v}/u_0, \quad w = \bar{w}/(Lu_0), \quad q = \bar{q}/u_0. \quad (2)$$

The flow region in the physical plane can be mapped into the w plane with the correspondence shown in Fig. 2.

Let $\Gamma(w)$ be the logarithm of the dimensionless complex velocity,

$$\Gamma(w) = \ln(dw/dz) = Q(\phi, \psi) - i\theta(\phi, \psi), \quad \text{where } Q = \ln q, \quad (3)$$

$\Gamma(w)$ will be an analytic function of w with Q, θ related by the Cauchy–Riemann equations, i.e.,

$$\frac{\partial Q}{\partial \psi} = \frac{\partial \theta}{\partial \phi}, \quad \frac{\partial Q}{\partial \phi} = -\frac{\partial \theta}{\partial \psi}, \quad (4)$$

and both Q and θ will satisfy Laplace’s equation

$$\frac{\partial^2 Q}{\partial \phi^2} + \frac{\partial^2 Q}{\partial \psi^2} = \frac{\partial^2 \theta}{\partial \phi^2} + \frac{\partial^2 \theta}{\partial \psi^2} = 0. \quad (5)$$

The boundary conditions of the wave problem will now be discussed.

a. Boundary Condition on the Free Streamline

We apply Bernoulli’s equation on the free streamline $\psi = 0$, i.e.,

$$\bar{p} + \frac{1}{2}\rho\bar{q}^2 = p_0 + \frac{1}{2}\rho u_0^2, \quad (6)$$

where ρ is the constant fluid density. The fluid pressure \bar{p} just inside the free surface and the constant pressure p_0 of the surroundings are related by Laplace’s formula

$$p_0 - \bar{p} = T/\bar{R}_f. \quad (7)$$

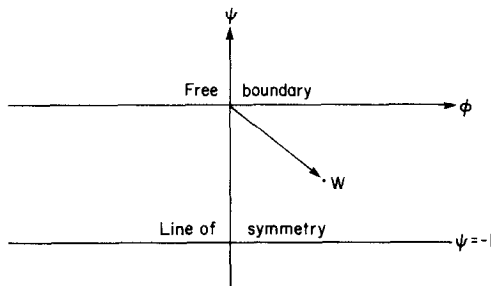


FIG. 2. The w plane.

Here T is the surface tension coefficient and $R_f = \bar{R}_f/L$ is the nondimensional radius of curvature of the free streamline, i.e.,

$$R_f^{-1} = \frac{\partial \theta}{\partial s} = q \frac{\partial \theta}{\partial \phi}, \tag{8}$$

where ds is the differential arc length along the free streamline. If we substitute (7) and (8) into (6), we obtain after some manipulations,

$$\frac{\partial \theta}{\partial \phi} = \frac{1}{2} \alpha (q - q^{-1}) \quad \text{on } \psi = 0, \tag{9}$$

where $\alpha = \rho u_0^2 L/T$ is the Weber number. Putting $q = e^Q$ and using (4), we find

$$\frac{\partial Q}{\partial \psi} = \alpha \sinh Q \quad \text{on } \psi = 0. \tag{10}$$

b. Boundary Condition on the Line of Symmetry

On the line of symmetry $\psi = -1$, the fluid deflection angle is constant, i.e., $\theta = 0$; hence $\partial \theta / \partial \phi = 0$. Using (4), this yields

$$\frac{\partial Q}{\partial \psi} = 0 \quad \text{on } \psi = -1. \tag{11}$$

c. Periodicity of Q in the w Plane

It is shown in Appendix A that $Q(\phi, \psi)$ is periodic with respect to ϕ . If the wavelength of Q in the w plane is defined to be λ , we can impose the periodic boundary condition, i.e.,

$$Q(\phi, \psi) = Q(\phi + \lambda, \psi). \tag{12}$$

Collecting all the results, we have the nonlinear problem¹

$$\frac{\partial^2 Q}{\partial \phi^2} + \frac{\partial^2 Q}{\partial \psi^2} = 0, \quad -1 \leq \psi \leq 0, \quad S \leq \phi \leq S + \lambda, \tag{13a}$$

$$\frac{\partial Q}{\partial \psi} = \alpha \sinh Q \quad \text{on } \psi = 0, \tag{13b}$$

$$\frac{\partial Q}{\partial \psi} = 0 \quad \text{on } \psi = -1, \tag{13c}$$

¹ Note our nondimensionalization is different from that used by Crapper so that the Weber number α appears explicitly here in the nonlinear boundary condition (13b); thus ψ varies from -1 to 0 for all values of α .

$$Q(\phi, \psi) = Q(\phi + \lambda, \psi), \quad -1 \leq \psi \leq 0, \tag{13d}$$

where S is an arbitrary constant.

We should note that this problem is translationally invariant with respect to ϕ , and we may define the problem in the domain $(-1 \leq \psi \leq 0, 0 \leq \phi \leq \lambda)$. The nonlinear capillary wave problem is displayed in Fig. 3 and it can be verified that $Q = 0$ is a solution of the boundary value problem. However, when λ satisfies a dispersion equation, to be derived later, there are also nontrivial solutions which we will determine using a numerical method.

The derivation of an exact solution for the boundary value problem in Fig. 3 is given in Appendix A; here we present the solution as follows:

$$Q = \ln \left\{ \frac{1 + (\kappa \operatorname{sn}(\gamma\phi, \kappa)/\operatorname{dn}[\gamma(\psi + 1), \kappa'])}{1 - (\kappa \operatorname{sn}(\gamma\phi, \kappa)/\operatorname{dn}[\gamma(\psi + 1), \kappa'])} \right\}, \tag{14}$$

$$\alpha = \gamma\kappa'^2 \frac{\operatorname{sn}(\gamma, \kappa') \operatorname{cn}(\gamma, \kappa')}{\operatorname{dn}(\gamma, \kappa')}, \tag{15}$$

where sn , cn , and dn are the Jacobian elliptic functions in standard notation [18] and κ is the modulus. Here γ , which is proportional to the wave number, and the complementary modulus κ' are related by dispersion formula (15). Moreover, γ must satisfy the inequality

$$0 < \gamma < K', \tag{16}$$

to prevent the denominator of (14) from vanishing. Here K' is the complementary elliptic integral of the first kind.

The period of the elliptic function sn is $4K$, where K is the elliptic integral of the first kind; thus we obtain from (14)

$$\gamma(\phi + \lambda) - \gamma\phi = 4K. \tag{17}$$

Thus the wavelength λ of Q in the w plane is given by

$$\lambda = 4K/\gamma. \tag{18}$$

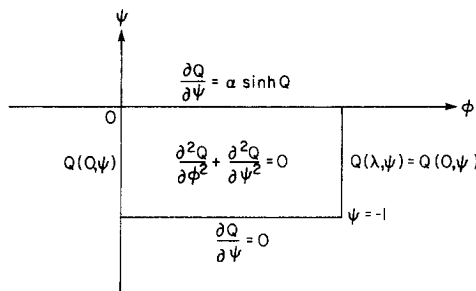


FIG. 3. Nonlinear capillary wave problem.

3. NUMERICAL PROCEDURE TO SOLVE THE CAPILLARY WAVE PROBLEM

To solve the capillary wave problem shown in Fig. 3 numerically, we introduce a grid on the rectangular domain by selecting two integers M and N and defining the grid sizes $h = \lambda/M$, $k = 1/N$, then

$$\begin{aligned} \phi_i &= (i - 1)h, & i &= 1, 2, \dots, M, \\ \psi_j &= -1 + jk, & j &= 0, 1, \dots, N. \end{aligned} \tag{19}$$

The grid is shown in Fig. 4. Note that the rectangle defined by the solid lines is the domain of integration.

Centered second-order differences will be used to approximate the derivatives. After discretizing Laplace's equation with the standard five-point scheme, we obtain

$$\begin{aligned} Q_{i,j-1} + Q_{i,j+1} - 2(1 + \sigma)Q_{i,j} + \sigma(Q_{i-1,j} + Q_{i+1,j}) &= 0, \\ i &= 1, 2, \dots, M, \quad j = 0, 1, \dots, N, \end{aligned} \tag{20}$$

where $\sigma = (k/h)^2$ and $Q_{i,j}$ is an approximation for $Q(\phi_i, \psi_j)$.

Boundary conditions (13b) and (13c) require

$$Q_{i,N+1} = 2ak \sinh Q_{i,N} + Q_{i,N-1}, \quad i = 1, 2, \dots, M, \tag{21a}$$

$$Q_{i,-1} = Q_{i,1}, \quad i = 1, 2, \dots, M, \tag{21b}$$

and the periodicity condition (13d) yields

$$Q_{0,j} = Q_{M,j}, \quad j = 0, 1, \dots, N, \tag{21c}$$

$$Q_{M+1,j} = Q_{1,j}, \quad j = 0, 1, \dots, N. \tag{21d}$$

In (20), there are unknown values of Q which correspond to the points on the fictitious dotted lines shown in Fig. 4; these unknowns can be replaced by boundary and interior point values using (21).

If we combine (20) and (21), after placing the nonlinear unknown terms arising from (21a) on the right-hand side, we obtain a system of equations which can be written in the matrix form

$$\mathbf{B} \cdot \mathbf{Q} = \mathbf{b}, \tag{22}$$

where \mathbf{B} is the $(N + 1) \times (N + 1)$ matrix of block tridiagonal form

$$\mathbf{B} = \begin{pmatrix} \mathbf{A} & 2\mathbf{I} & & & & & \\ \mathbf{I} & \mathbf{A} & \mathbf{I} & & & & \\ & & & \ddots & & & \\ & & & & \mathbf{I} & \mathbf{A} & \mathbf{I} \\ & & & & & 2\mathbf{I} & \mathbf{A} \end{pmatrix}, \tag{23}$$

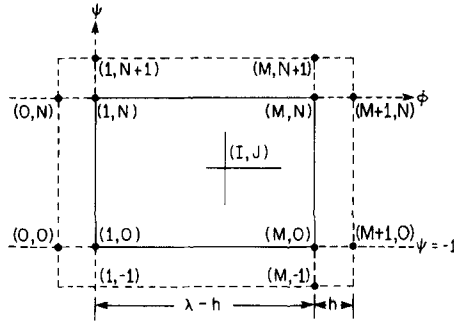


FIG. 4. Mesh for numerical integration.

I is the $M \times M$ identity matrix, and A is the $M \times M$ matrix

$$A = \begin{pmatrix} -2(1 + \sigma) & \sigma & & & \sigma \\ \sigma & -2(1 + \sigma) & \sigma & 0 & \\ & 0 & \ddots & \sigma & -2(1 + \sigma) & \sigma \\ \sigma & & & \sigma & -2(1 + \sigma) & \sigma \\ & & & & \sigma & -2(1 + \sigma) \end{pmatrix}, \quad (24)$$

Q and b are vectors in partitioned form

$$Q = \begin{pmatrix} Q_0 \\ Q_1 \\ \vdots \\ Q_{N-1} \\ Q_N \end{pmatrix}, \quad b = \begin{pmatrix} b_0 \\ b_1 \\ \vdots \\ b_{N-1} \\ b_N \end{pmatrix}, \quad (25)$$

with

$$Q_j = \begin{pmatrix} Q_{1,j} \\ Q_{2,j} \\ \vdots \\ Q_{M-1,j} \\ Q_{M,j} \end{pmatrix}, \quad j = 0, 1, \dots, N, \quad (26)$$

b_0, b_1, \dots, b_{N-1} are M th-order null vectors and

$$b_N = -2ak \begin{pmatrix} \sinh Q_{1,N} \\ \sinh Q_{2,N} \\ \vdots \\ \sinh Q_{M-1,N} \\ \sinh Q_{M,N} \end{pmatrix}. \quad (27)$$

Buneman's algorithm has been explained in detail by Buzbee *et al.* [3]; here we note two important facts about this method.

(i) If we want to solve (22) by Buneman's algorithm, the reduction process will eliminate the unknowns systematically until only the middle vector $\mathbf{Q}_{2^{m-1}}$ is left (here we assume $N = 2^m$ with m an integer for simplicity); thus $\mathbf{Q}_{2^{m-1}}$ is always the first vector to be determined.

(ii) During the process of reduction, all the right-hand side vectors corresponding to the reduced systems will be reconstructed; however, the middle vector $\mathbf{b}_{2^{m-1}}$ does not influence the reconstruction of the other right-hand side vectors.

If we want to take advantage of Buneman's algorithm and solve (22) efficiently, it would be desirable to have \mathbf{Q}_N and \mathbf{b}_N located in the middle of the array. This can be achieved by reflecting all the vectors above \mathbf{Q}_N to a position below it as shown in (28a):

$$\left(\begin{array}{ccccccc} \mathbf{A} & 2\mathbf{I} & & & & & \\ \mathbf{I} & \mathbf{A} & & \mathbf{I} & & & \\ & & \ddots & & \ddots & & \\ \hline & & & \mathbf{I} & \mathbf{A} & \mathbf{I} & \\ \hline & & & & & \ddots & \ddots \\ & & & & & \mathbf{I} & \mathbf{A} & \mathbf{I} \\ & & & & & & 2\mathbf{I} & \mathbf{A} \end{array} \right) \begin{pmatrix} \mathbf{Q}_0 \\ \mathbf{Q}_1 \\ \vdots \\ \mathbf{Q}_N \\ \vdots \\ \mathbf{Q}_1 \\ \mathbf{Q}_0 \end{pmatrix} = \begin{pmatrix} \mathbf{b}_0 \\ \mathbf{b}_1 \\ \vdots \\ \mathbf{b}_N \\ \vdots \\ \mathbf{b}_1 \\ \mathbf{b}_0 \end{pmatrix}. \tag{28a}$$

If we define the corresponding matrix and vectors in (28a) to be \mathbf{B}' , \mathbf{Q}' , and \mathbf{b}' , respectively, then we have

$$\mathbf{B}' \cdot \mathbf{Q}' = \mathbf{b}', \tag{28b}$$

and the order of the matrix \mathbf{B}' is $(2N + 1)$. Now we solve the system of equations (28) by Buneman's algorithm, noting that \mathbf{b}_N is the middle vector, and all the nonlinear terms in \mathbf{b}_N will not influence the other right-hand side vectors during the course of the reduction.

To apply Buneman's algorithm on (28), we will have to compute the sequence $\{\mathbf{p}_j^{(r)}, \mathbf{q}_j^{(r)}\}, j = 0, 1, \dots, 2N + 1, r = 1, 2, \dots, m + 1$. Due to the symmetry of system (28), the computation of $\{\mathbf{p}_j^{(r)}, \mathbf{q}_j^{(r)}\}$ for $j > N$ is not required. Moreover, all the right-hand side vectors in (28) are null vectors except \mathbf{b}_N ; this implies that all $\{\mathbf{p}_j^{(r)}, \mathbf{q}_j^{(r)}\}, j = 0, 1, \dots, N - 1, r = 1, 2, \dots, m$ are null vectors for this particular problem. Thus, we start the reduction directly by constructing $\{\mathbf{p}_N^{(r)}, \mathbf{q}_N^{(r)}\}, r = 1, 2, \dots, m + 1$. Given an initial guess for \mathbf{Q}_N , say $\mathbf{Q}_N^{(0)}$, we start by constructing $\{\mathbf{p}_N^{(r)}, \mathbf{q}_N^{(r)}\}$. The final equation of the reduction will be

$$\mathbf{C}^{(m+1)}(\mathbf{Q}_N - \mathbf{p}_N^{(m+1)}) = \mathbf{q}_N^{(m+1)}, \tag{29}$$

or

$$\mathbf{Q}_N = \mathbf{p}_N^{(m+1)} + \mathbf{C}^{(m+1)^{-1}} \mathbf{q}_N^{(m+1)}, \quad (30)$$

where

$$\mathbf{C}^{(m+1)} = - \prod_{j=1}^{2^{m+1}} (\mathbf{A} + 2 \cos \theta_j^{(m+1)} \mathbf{I}), \quad (31)$$

and

$$\theta_j^{(m+1)} = j\pi/2^m, \quad j = 1, 2, \dots, 2^{m+1}. \quad (32)$$

Since $\mathbf{p}_N^{(m+1)}$ and $\mathbf{q}_N^{(m+1)}$ are functions of $\mathbf{Q}_N^{(0)}$, Eq. (30) can be written in the form

$$\mathbf{Q}_N = \mathbf{F}(\mathbf{Q}_N^{(0)}), \quad (33)$$

where

$$\mathbf{F}(\mathbf{Q}_N^{(0)}) = \mathbf{p}_N^{(m+1)} + \mathbf{C}^{(m+1)^{-1}} \mathbf{q}_N^{(m+1)}. \quad (34)$$

We solve (29) or (33) for \mathbf{Q}_N , and once \mathbf{Q}_N is known, denoting it by $\mathbf{Q}_N^{(l)}$, we may check if $\|\mathbf{Q}_N^{(l)} - \mathbf{Q}_N^{(0)}\|$ is less than a given tolerance. If the tolerance is met, all the remaining unknowns can be back-solved directly; if not, we replace $\mathbf{Q}_N^{(0)}$ by $\mathbf{Q}_N^{(l)}$ and repeat the process until convergence is achieved.

There are several problems with the above algorithm, namely:

(i) Placing the nonlinear unknown terms on the right-hand side of (22) implies that the nonlinear boundary condition is treated as a Neumann-type boundary condition; thus, the matrix \mathbf{B} is formulated as if we were solving Laplace's equation with Neumann and periodic boundary conditions. It is well known that such a matrix is singular. Moreover, \mathbf{B}' in (28) is also singular. The singular nature of \mathbf{B}' can be verified by choosing a vector \mathbf{e} of the form

$$\mathbf{e}^T = [\bar{\mathbf{e}}, \bar{\mathbf{e}}, \dots, \bar{\mathbf{e}}]_{(2N+1)}, \quad (35)$$

with

$$\bar{\mathbf{e}}^T = [1, 1, \dots, 1]_M, \quad (36)$$

and noting that

$$\mathbf{B}' \cdot \mathbf{e} = \mathbf{0}. \quad (37)$$

Thus any constant multiple of \mathbf{e} is a nontrivial homogeneous solution of (28).

(ii) We can not specify the phase of the capillary wave from the numerical formulation of problem (22) since it is translationally invariant; however, it is

desirable to fix the phase to make a comparison of the numerical solution with the known exact solution.

(iii) Algorithm (33) is basically a fixed point iteration which may not converge since hyperbolic sines are involved in the nonlinear terms and they have large slopes.

First, we consider the difficulties (i) and (ii) together.

The necessary and sufficient condition for system (28) to have a solution is given by the Fredholm alternative [6], i.e.,

$$\mathbf{b}'^T \cdot \mathbf{e} = 0. \quad (38)$$

Since \mathbf{b}'_N is the only nonzero forcing vector, (38) reduces to

$$\sum_{i=1}^M \sinh Q_{i,N} = 0. \quad (39)$$

We should note that Green's theorem requires

$$\oint_C \frac{\partial Q}{\partial n} ds = 0, \quad (40)$$

to obtain a source-free solution of Laplace's equation. Carrying (40) out numerically by the trapezoidal rule for the problem formulated in Fig. 3 yields the same result (39).

It is important to note that if a singular linear system of equations has solutions, the solutions will not be unique, for a new solution can be generated by adding a solution of the corresponding homogeneous system to an existing solution. However, the above statement is not valid for this particular wave problem because \mathbf{b}' in (28) depends on nonlinear unknown terms. Adding any constant multiple of \mathbf{e} to an existing solution of (28) will not produce a new solution because (39) will not be satisfied.

Owing to the fact that the nonlinear wave problem is translationally invariant with respect to ϕ , the numerical solution of (28) may have an infinite number of different phases depending on the initial guess $\mathbf{Q}_N^{(0)}$. However, the phase of the wave can be fixed by imposing a value $Q_{i,N}$ at a given point on the free streamline. The simplest choice and the one that makes the comparison of the exact solution with the numerical solution easiest, is to choose $Q = 0$ at the first grid point on the free streamline, i.e., $Q_{1,N} = 0$. It is shown in Appendix B that once a numerical solution of (28) is obtained, it can be used to generate $M - 1$ additional solutions with different phases.

The following procedure for solving the singular system (28) will indicate how the phase of the wave may be fixed, i.e., each time we perform the fixed point iteration (33), we will choose a vector $\mathbf{Q}_N^{(i)}$ such that $\mathbf{Q}_N^{(i)}$ is forced to satisfy (39) and to have a fixed phase.

To show how the singularity in \mathbf{B}' is handled, we define

$$\mathbf{G}_j \equiv \mathbf{A} + 2 \cos \theta_j^{(m+1)} \mathbf{I}, \quad (41)$$

and (31) yields

$$\mathbf{C}^{(m+1)} = - \prod_{j=1}^{2^{m+1}} \mathbf{G}_j. \quad (42)$$

Substituting (42) into (29), we obtain

$$\prod_{j=1}^{2^{m+1}} \mathbf{G}_j (\mathbf{Q}_N - \mathbf{p}_N^{(m+1)}) = -\mathbf{q}_N^{(m+1)}. \quad (43)$$

To solve (43), we put $\mathbf{Z}_1 = -\mathbf{q}_N^{(m+1)}$ and repeatedly solve

$$\mathbf{G}_j \mathbf{Z}_{j+1} = \mathbf{Z}_j, \quad j = 1, 2, \dots, 2^{m+1}, \quad (44)$$

for \mathbf{Z}_j , $j > 1$. Since \mathbf{G}_j is a matrix of nearly tridiagonal form with nonzero elements in the upper right and lower left corners, we adopt the rank-one method [23, 24] to solve system (44). However, when we reach the last step of (44), i.e., $j = 2^{m+1}$, we find $\cos \theta_j^{(m+1)} = 1$, and from (41)

$$\mathbf{G}_{2^{m+1}} = \mathbf{A} + 2\mathbf{I} \quad (45a)$$

$$= \begin{pmatrix} -2\sigma & \sigma & & & \sigma \\ \sigma & -2\sigma & \sigma & & 0 \\ & & \ddots & \ddots & \\ & 0 & \sigma & -2\sigma & \sigma \\ \sigma & & & \sigma & -2\sigma \end{pmatrix}, \quad (45b)$$

which is a singular matrix. Therefore at the last step we must solve the singular system

$$\mathbf{G}_{2^{m+1}} \mathbf{Z}_{2^{m+1}+1} = \mathbf{Z}_{2^{m+1}}, \quad (46)$$

where $\mathbf{Z}_{2^{m+1}+1}$ is defined as

$$\mathbf{Z}_{2^{m+1}+1} \equiv \mathbf{Q}_N^{(t)} - \mathbf{p}_N^{(m+1)}. \quad (47)$$

Substituting (47) into (46), we obtain after rearranging the equation

$$\mathbf{G}_{2^{m+1}} \mathbf{Q}_N^{(t)} = \tilde{\mathbf{Z}}, \quad (48)$$

where $\tilde{\mathbf{Z}}$ is defined as

$$\tilde{\mathbf{Z}} \equiv \mathbf{G}_{2^{m+1}} \mathbf{p}_N^{(m+1)} + \mathbf{Z}_{2^{m+1}}, \quad (49)$$

which is a known vector. The nonzero vector $\bar{\mathbf{e}}$ defined in (36) is a solution of the equation

$$\mathbf{G}_{2m+1} \bar{\mathbf{e}} = \mathbf{0}. \tag{50}$$

Thus, the necessary and sufficient condition for (48) to have a solution is

$$\tilde{\mathbf{Z}}^T \bar{\mathbf{e}} = 0. \tag{51}$$

If we denote the elements of $\tilde{\mathbf{Z}}$ to be

$$\tilde{\mathbf{Z}}^T \equiv [\bar{Z}_1, \bar{Z}_2, \dots, \bar{Z}_M], \tag{52}$$

then (51) requires

$$\sum_{i=1}^M \bar{Z}_i = 0, \tag{53}$$

for a solution to exist.

As discussed previously, it is desirable to fix the phase of the wave by assigning a specific element of $\mathbf{Q}_N^{(t)}$ to be zero for this problem. We shall choose the first element of $\mathbf{Q}_N^{(t)}$, $Q_{1,N}^{(t)}$ to be zero. Once $Q_{1,N}^{(t)}$ is chosen, the solution of (48) will be unique and we can determine the solution in the following way:

We multiply both sides of (48) by a nonsingular matrix [6] which is obtained by replacing the first row of the $M \times M$ identity matrix by the vector $\bar{\mathbf{e}}$. After performing the multiplication, we obtain a new system

$$\mathbf{G}'_{2m+1} \mathbf{Q}_N^{(t)} = \tilde{\mathbf{Z}}^t, \tag{54}$$

where \mathbf{G}'_{2m+1} remains the same as \mathbf{G}_{2m+1} except the elements of the first row are zero, and

$$\tilde{\mathbf{Z}}^t = \left[\sum_{i=1}^M \bar{Z}_i, \bar{Z}_2, \dots, \bar{Z}_M \right], \tag{55a}$$

$$= [0, \bar{Z}_2, \dots, \bar{Z}_M], \tag{55b}$$

where we have used result (53). We can now delete the first equation of (54) and since $Q_{1,N}^{(t)}$ is fixed to be zero, we may also delete the first column of \mathbf{G}'_{2m+1} ; the remaining matrix is of tridiagonal form. Now the contracted system of order $(M - 1)$ is no longer singular and we can solve for $Q_{i,N}^{(t)}$, $i = 2, 3, \dots, M$.

To satisfy (39), while keeping the first element $Q_{1,N}^{(t)}$ equal to zero, we must choose a constant δ , such that

$$\sum_{i=2}^M \sinh(Q_{i,N}^{(t)} + \delta) = 0. \tag{56}$$

After δ is determined from (56), we add δ to $Q_{i,N}^{(l)}$, $i = 2, 3, \dots, M$ while keeping $Q_{1,N}^{(l)}$ zero. The new $\mathbf{Q}_N^{(l)}$ is forced to satisfy (39) and the phase of the wave has been fixed since the first element $Q_{1,N}^{(l)}$ is zero. Therefore, we have removed difficulties (i) and (ii).

The remaining difficulty (iii) can be handled by applying Newton's method to accelerate the convergence of (33). Using (33), we define

$$\mathbf{H}(\mathbf{Q}_N) \equiv \mathbf{Q}_N - \mathbf{F}(\mathbf{Q}_N) = \mathbf{0}. \quad (57)$$

Applying Newton's method, we obtain the following equation

$$\mathbf{J}_H(\mathbf{Q}_N^{(1)} - \mathbf{Q}_N^{(0)}) = -\mathbf{H}(\mathbf{Q}_N^{(0)}) = \mathbf{F}(\mathbf{Q}_N^{(0)}) - \mathbf{Q}_N^{(0)}, \quad (58)$$

where \mathbf{J}_H is the Jacobian matrix, defined as

$$\mathbf{J}_H \equiv \frac{\partial \mathbf{H}_j(\mathbf{Q}_N)}{\partial Q_{i,N}} = \mathbf{I} - \frac{\partial \mathbf{F}_j(\mathbf{Q}_N)}{\partial Q_{i,N}}, \quad (59)$$

and \mathbf{I} is the $M \times M$ identity matrix. Since we do not have an explicit expression for $\mathbf{F}(\mathbf{Q}_N)$, we have to approximate the Jacobian matrix numerically.

First we choose an appropriate initial guess $\mathbf{Q}_N^{(0)}$ to perform the fixed point iteration (33) as discussed above and obtain $\mathbf{Q}_N^{(l)}$. Next we add a small number ε to each of the elements of $\mathbf{Q}_N^{(0)}$ and repeat (33) to obtain

$$\mathbf{Q}_N(i, \varepsilon) = \mathbf{F}(Q_{1,N}^{(0)}, Q_{2,N}^{(0)}, \dots, Q_{i,N}^{(0)} + \varepsilon, \dots, Q_{M,N}^{(0)}). \quad (60)$$

The i th column on the Jacobian matrix is computed as

$$\mathbf{J}_{H,i} = \mathbf{I}_i - \varepsilon^{-1}(\mathbf{Q}_N(i, \varepsilon) - \mathbf{Q}_N^{(l)}), \quad (61)$$

where \mathbf{I}_i is the i th column of the identity matrix \mathbf{I} .

After we obtain the Jacobian matrix, we solve (58) for $\mathbf{Q}_N^{(1)}$. If $\|\mathbf{Q}_N^{(1)} - \mathbf{Q}_N^{(0)}\|$ is smaller than a given tolerance, which we chose to be 1.0×10^{-10} for all cases, we back solve for the remaining unknowns; if not, we replace $\mathbf{Q}_N^{(0)}$ by $\mathbf{Q}_N^{(1)}$ and repeat the iteration procedure. The back substitution process is straightforward, and the reader may refer to Buzbee *et al.* [3] and Liu [24].

Since Newton's method requires considerable computer time to evaluate the Jacobian matrix, we computed the Jacobian matrix once and then used a method proposed by Broyden [24, 25] to update the Jacobian matrix. This procedure has proven to be very successful.

We summarize our numerical algorithm as follows:

- (1) Given the initial guess $\mathbf{Q}_N^{(0)}$, compute $\mathbf{p}_N^{(r)}$, $\mathbf{q}_N^{(r)}$, $r = 1, 2, \dots, m + 1$.
- (2) Perform the fixed point iteration (33) to obtain $\mathbf{Q}_N^{(l)}$.
- (3) Construct the Jacobian matrix using (60) and (61).
- (4) Solve (58) for $\mathbf{Q}_N^{(1)}$.

(5) Check convergence. If the tolerance is met, go to (8) below; otherwise continue as follows:

- (6) Update the Jacobian matrix by Broyden's method.
- (7) Replace $\mathbf{Q}_N^{(0)}$ by $\mathbf{Q}_N^{(1)}$, repeat (1), (2), (4), and (5).
- (8) Back-solve directly for the remaining unknowns.

4. COMPARISON OF NUMERICAL SOLUTION WITH EXACT SOLUTION

We chose two cases for comparison; one case corresponds to long waves and the other to short waves. The variables for these two cases satisfy (15) and are specified as

$$\text{Case I:} \quad \text{long waves} \quad \alpha = 0.7239937, \quad \kappa = 0.3, \quad \lambda = 6.$$

$$\text{Case II:} \quad \text{short waves} \quad \alpha = 11.801483, \quad \kappa = 1.0 \times 10^{-6}, \quad \lambda = 0.45.$$

To avoid the trivial solution, $Q = 0$, the initial guess for \mathbf{Q}_N cannot be very small, or the zero solution will result. An initial guess of magnitude one is recommended. Attempts were also made to choose some arbitrary wavelengths λ for Cases I and II such that dispersion relation (15) is not satisfied; however, only trivial solutions were obtained in those cases, as expected.

For each case, we chose two sets of mesh sizes (h, k) , so that we could perform a Richardson's extrapolation to obtain solutions with fourth-order accuracy. The computations were performed on an IBM 360/65 machine with double precision arithmetic. The exact solution of these two cases can be computed using (14). Since the wave is symmetric, we only present the results of a quarter wavelength on the free surfaces. The comparisons for Cases I and II are shown in Tables I and II, respectively. Numerical results for the long waves are very accurate while for the short waves, the errors are larger than expected. In the latter cases the amplitude of Q is not small and the wavelength is extremely short, so that the larger errors are due to the steepness of the wave; thus, the truncated fourth-order derivatives are not insignificant compared with the errors $O(h^2, k^2)$. Nevertheless, the ratio of errors (D_1/D_2) still remains almost 4 for every point when the mesh sizes are reduced by a factor of two.

It is also interesting to compare the rate of convergence and the computation times of Newton's method and Broyden's method. With all the parameters specified as in Case I-1 (see Table I), we made two computations using these different methods. Both methods gave identical numerical solutions. Since Newton's method should have a quadratic rate of convergence, we can check the values of f_n such that

$$\varepsilon_{n+1} = f_n \varepsilon_n^2, \quad (62)$$

where ε_n is the error of the n th iteration measured from the final frozen value. We

TABLE I
Numerical Results of Long Wave Case

ϕ	Exact	I-1	D_1^a	I-2	D_2	I-3	D_3	D_1/D_2^b
0.2	0.1976749	0.1962304	7.5186×10^{-4}	0.1974913	1.8355×10^{-4}	0.1976808	5.88×10^{-6}	4.096
0.4	0.3891822	0.3876543	1.5068×10^{-3}	0.3888139	3.6830×10^{-4}	0.3891934	1.12×10^{-5}	4.091
0.6	0.5678540	0.5655958	2.2582×10^{-3}	0.5673009	5.5311×10^{-4}	0.5678693	1.53×10^{-5}	4.0828
0.8	0.7261859	0.7232048	2.9811×10^{-3}	0.7254537	7.3220×10^{-4}	0.7262033	1.74×10^{-5}	4.0712
1.0	0.8558823	0.8522569	3.6254×10^{-3}	0.8549987	8.9355×10^{-4}	0.8558793	1.71×10^{-5}	4.057
1.2	0.9485252	0.9444052	4.1200×10^{-3}	0.9475065	1.0186×10^{-4}	0.9485403	1.52×10^{-5}	4.0446
1.4	0.9969473	0.9925561	4.3913×10^{-3}	0.9958594	1.0879×10^{-4}	0.9969605	1.32×10^{-5}	4.0365
1.5	1.003106	—	—	1.002009	1.0970×10^{-4}	—	—	—

Note. Case I: $\alpha = 0.72399337, k = 0.3, \lambda = 6$; Case I-1: $(h_1, k_1) = (0.2, 0.125), O(h_1^2) = 0.04$; Case I-2: $(h_2, k_2) = (0.1, 0.0625), O(h_2^2) = 0.01$; and Case I-3: Results of Richardson's extrapolation, $O(h_3^2) = 0.0016$.

^a D_1, D_2, D_3 refer to the differences between exact solution and the three cases.

^b For results with second order accuracy, this quotient should be 4.

TABLE II
Numerical Results of Short Wave Case

ϕ	Exact	II-1	D_1	II-2	D_2	II-3	D_3	D_1/D_2
0.015	0.223145750	0.226285002	3.13925×10^{-3}	0.2239958262	8.12456×10^{-4}	0.223182607	3.8657×10^{-5}	3.86390
0.03	0.441784373	0.447938490	6.15411×10^{-3}	0.443377063	1.59268×10^{-3}	0.441856883	7.2211×10^{-5}	3.86398
0.045	0.650229337	0.659120158	8.89082×10^{-3}	0.652528170	2.29883×10^{-3}	0.650330840	1.0150×10^{-4}	3.86753
0.06	0.840525043	0.851690912	1.11659×10^{-2}	0.843403035	2.87799×10^{-3}	0.840640409	1.1537×10^{-4}	3.87975
0.075	1.001791755	1.014611062	1.28193×10^{-2}	1.005074270	3.28252×10^{-3}	1.001895339	1.0358×10^{-4}	3.90533
0.09	1.120771982	1.134578116	1.38061×10^{-2}	1.124274786	3.50280×10^{-3}	1.120840743	6.8361×10^{-5}	3.94145
0.105	1.184446033	1.198676873	1.42308×10^{-2}	1.188031768	3.58414×10^{-3}	1.184481277	3.5244×10^{-5}	3.97050
0.1125	1.19262421	—	—	1.19621666	3.59265×10^{-3}	—	—	—

Note. Case II: $\alpha = 11.801483$, $k = 1.0 \times 10^{-6}$, $\lambda = 0.45$; Case II-1: $(h_1, k_1) = (0.015, 0.015625)$, $O(k_1^2) = 2.4414 \times 10^{-4}$; Case II-2: $(h_2, k_2) = (0.0075, 0.0078125)$, $O(k_2^2) = 6.1035 \times 10^{-5}$; and Case II-3: Results of Richardson's extrapolation, $O(k_3^1) = O(0.015625^4) = 5.96 \times 10^{-8}$.

TABLE III
Comparison of Newton's Method with Broyden's Method

No. of iteration	Newton's method			Broyden's method		
	Num. value	ϵ_n	f_n	Num. value	ϵ_n	f_n
1	1.231781095975	0.239225	1.746	1.231781095975	0.239225	1.647
2	1.086790337780	0.942343×10^{-1}	1.190	1.086790315518	0.94234×10^{-1}	3.692
3	1.003124579696	0.105690×10^{-1}	1.583	1.025343812851	0.32788×10^{-1}	3.429
4	0.992732894213	0.17684×10^{-3}	1.589	0.996242280951	0.36862×10^{-2}	16.348
5	0.992556099890	0.497×10^{-7}		0.992778187871	0.22214×10^{-3}	-95.283
6	Frozen			0.992551358503	-0.46921×10^{-5}	
7				0.992556652092	0.60191×10^{-6}	
8				0.992556514961	0.46478×10^{-6}	
9				0.992555330629	-0.71956×10^{-6}	
10				0.992556048619	0.15625×10^{-8}	
11				0.992556050143	0.336×10^{-10}	
12				0.992556050184	0.26×10^{-11}	
13				Frozen		

Note. $a = 0.72399337$, $k = 0.3$, $\lambda = 6$, $(h, k) = (0.2, 0.125)$, frozen value: 0.9925560501815 ($\phi, \psi) = (1.4, 0)$.

took one point on the free streamline from Table I for the comparison, and the numerical results are shown in Table III.

We observe that Newton's method does indicate a quadratic rate of convergence. In this example, there are 270 unknowns in the grid. The 30 points which are on the free streamline are determined by the iteration while the remaining 240 points are back-solved directly. Although Broyden's method requires more iterations, it uses considerably less computing time. Newton's method required 80 sec of CPU time while Broyden's method required 29 sec of CPU time.

5. CONCLUSION

Numerical solutions of elliptic partial differential equations with nonlinear boundary conditions using finite difference methods are rarely found in the literature. Our development offers an accurate and efficient method to solve Laplace's equation with a nonlinear boundary condition. The discretized system of the capillary wave problem can be reduced to a set of nonlinear algebraic equations involving unknowns only on the nonlinear boundary line. Newton's method is used to determine the unknowns and the remaining boundary and interior points are determined directly. This method has also been applied to solve the two-dimensional potential flow of a jet emanating from a slot with surface tension effects taken into account [26]. In this case we must handle a split boundary condition, i.e., the normal derivative is specified in two parts on an infinite line, with one part being nonlinear.

Some generalizations of our method are presented here.

(i) The method is applicable to a nonlinear boundary condition on one side of a rectangular domain which has the form $\partial Q/\partial n = f(Q)$, where f is any nonlinear function of Q . Here we considered the special case $f(Q) = \alpha \sinh Q$ (see Eq. (13b)).

(ii) Owing to the special properties of the block cyclic reduction method, it is possible to solve a linear partial differential equation with *two* nonlinear boundary conditions on opposite sides of a rectangular domain. To be specific, consider the wave problem in this paper but with boundary condition (13c) replaced with a nonlinear boundary condition of the form $\partial Q/\partial n = g(Q)$, which might correspond to another free surface. After discretizing the governing equations and placing the nonlinear terms on the right-hand side, a new system (22) is obtained, similar to the previous system except \mathbf{b}_0 now depends on the unknown elements \mathbf{Q}_0 . We reflect the system as before and perform the reduction on (28). In this case we stop the reduction process one step before the final result (29), to obtain three equations resulting from the first, middle, and last equation of the array (28). The first and last equations will be identical due to the reflection. Thus, we have two equations involving the unknowns \mathbf{Q}_0 and \mathbf{Q}_N . It should be noted that the values of \mathbf{b}_0 and \mathbf{b}_N do not enter into the reconstruction of any of the other right-hand side vectors during the reduction process and thus the final two equations can be solved iteratively for \mathbf{Q}_0 and \mathbf{Q}_N . Once convergence is achieved, the remaining unknowns are computed

directly as in the previous case. This method fails if the two nonlinear boundary conditions are located on two adjacent sides of a rectangular domain.

(iii) Swarztrauber [10] has extended the block cyclic reduction method to solve separable elliptic equations. Since his method retains the special properties of the block cyclic reduction method discussed in Section 3, it should be possible to solve linear separable elliptic equations with nonlinear boundary conditions using the techniques developed in this paper.

APPENDIX A: DERIVATION OF AN EXACT SOLUTION FOR THE CAPILLARY WAVE PROBLEM

Consider the nonlinear capillary wave problem shown in Fig. 3:

$$\frac{\partial^2 Q}{\partial \phi^2} + \frac{\partial^2 Q}{\partial \psi^2} = 0, \quad -1 \leq \psi \leq 0, \quad 0 \leq \phi \leq \lambda, \quad (\text{A1a})$$

$$\frac{\partial Q}{\partial \psi} = \alpha \sinh Q \quad \text{on } \psi = 0, \quad (\text{A1b})$$

$$\frac{\partial Q}{\partial \psi} = 0 \quad \text{on } \psi = -1, \quad (\text{A1c})$$

$$Q(\phi, \psi) = Q(\phi + \lambda, \psi), \quad -1 \leq \psi \leq 0. \quad (\text{A1d})$$

An exact solution for capillary waves on a fluid of infinite depth was first derived by Crapper [16]. In his case, boundary condition (A1c) is replaced by

$$Q \rightarrow 0 \quad \text{as } \psi \rightarrow -\infty. \quad (\text{A2})$$

Crapper assumed that Q satisfied the condition

$$\frac{\partial Q}{\partial \psi} = f(\psi) \sinh Q, \quad (\text{A3})$$

for all (ϕ, ψ) . This leads to a solution involving only elementary trigonometric functions. Later Kinnersley [17] solved problem (A1) for finite fluid depths using the same assumption (A3). If we substitute (A3) into (A1b) and (A1c), we find

$$f(0) = \alpha, \quad (\text{A4a})$$

$$f(-1) = 0. \quad (\text{A4b})$$

We can integrate (A3) to obtain

$$\ln \tanh(Q/2) = F(\psi) + G(\phi), \quad (\text{A5})$$

where

$$\frac{dF(\psi)}{d\psi} = f(\psi), \quad (\text{A6})$$

and $G(\phi)$ is arbitrary; thus

$$Q = \ln \left\{ \frac{1 + X(\phi) Y(\psi)}{1 - X(\phi) Y(\psi)} \right\}, \quad (\text{A7})$$

where

$$X(\phi) = e^{G(\phi)}, \quad (\text{A8})$$

$$Y(\psi) = e^{F(\psi)}. \quad (\text{A9})$$

After substituting (A7) into (A1a), we find that $X(\phi)$ and $Y(\psi)$ must satisfy the two nonlinear differential equations

$$(X'(\phi))^2 = -a_1 - a_2 X^2(\phi) - a_3 X^4(\phi), \quad (\text{A10})$$

$$(Y'(\psi))^2 = a_3 + a_2 Y^2(\psi) + a_1 Y^4(\psi), \quad (\text{A11})$$

where a_1 , a_2 , and a_3 are constants. The solutions of (A10) and (A11) are expressible in terms of elliptic functions.

To fix ideas, consider the case where Q is small resulting from $X(\phi) Y(\psi)$ being small; we can approximate Q from (A7) by

$$Q \sim 2X(\phi) Y(\psi) \quad \text{for} \quad X(\phi) Y(\psi) \rightarrow 0. \quad (\text{A12})$$

We differentiate (A10) to obtain

$$X''(\phi) = -a_2 X(\phi) - 2a_3 X^3(\phi). \quad (\text{A13})$$

Assuming $X(\phi)$ is small, we can neglect the cubic term in (A13), and a_2 must be positive to obtain a solution which is bounded and periodic. To obtain real solutions for $X(\phi)$ and $Y(\psi)$, a_1 , a_2 , and a_3 cannot all have the same sign. With these restrictions we limit our choices of a_1 , a_2 , and a_3 to three, which are

$$\text{Case I:} \quad a_1 < 0, \quad a_2 > 0, \quad a_3 > 0,$$

$$\text{Case II:} \quad a_1 > 0, \quad a_2 > 0, \quad a_3 < 0,$$

$$\text{Case III:} \quad a_1 < 0, \quad a_2 > 0, \quad a_3 < 0.$$

After analyzing the three cases, we find that only Case I yields satisfactory solutions. The exact solution is given in (14). Substituting (14) into (A3) and (A4), we obtain dispersion formula (15).

APPENDIX B: GENERATION OF NEW SOLUTIONS FROM THE EXISTING SOLUTION OF EQ. (28)

Equation (28) can be rearranged in the form

$$\bar{\mathbf{B}}' \cdot \bar{\mathbf{Q}}' = \bar{\mathbf{b}}', \tag{B1}$$

where $\bar{\mathbf{B}}'$ is the $M \times M$ block matrix of the following form

$$\bar{\mathbf{B}}' = \begin{pmatrix} \bar{\mathbf{A}} & \sigma \bar{\mathbf{I}} & & \sigma \bar{\mathbf{I}} \\ \sigma \bar{\mathbf{I}} & \bar{\mathbf{A}} & \sigma \bar{\mathbf{I}} & \mathbf{0} \\ & & \vdots & \\ \mathbf{0} & \sigma \bar{\mathbf{I}} & \bar{\mathbf{A}} & \sigma \bar{\mathbf{I}} \\ \sigma \bar{\mathbf{I}} & & \sigma \bar{\mathbf{I}} & \bar{\mathbf{A}} \end{pmatrix}, \tag{B2}$$

$\bar{\mathbf{I}}$ is the $(2N + 1) \times (2N + 1)$ identity matrix and $\bar{\mathbf{A}}$ is the $(2N + 1) \times (2N + 1)$ triagonal matrix

$$\bar{\mathbf{A}} = \begin{pmatrix} -2(1 + \sigma) & 2 & & & & & & \\ 1 & -2(1 + \sigma) & 1 & & & & & \\ & & \ddots & \ddots & & & & \\ & & & 1 & & & & \\ & & & & -2(1 + \sigma) & 1 & & \\ & & & & 2 & & -2(1 + \sigma) & \\ & & & & & & & \end{pmatrix}, \tag{B3}$$

$\bar{\mathbf{Q}}'$ and $\bar{\mathbf{b}}'$ are vectors in partitioned form

$$\bar{\mathbf{Q}}' = \begin{pmatrix} \bar{Q}_1 \\ \bar{Q}_2 \\ \vdots \\ \bar{Q}_{M-1} \\ \bar{Q}_M \end{pmatrix}, \quad \bar{\mathbf{b}}' = \begin{pmatrix} \bar{b}_1 \\ \bar{b}_2 \\ \vdots \\ \bar{b}_{M-1} \\ \bar{b}_M \end{pmatrix}, \tag{B4}$$

and

$$\bar{Q}_l = \begin{pmatrix} Q_{l,0} \\ Q_{l,1} \\ \vdots \\ Q_{l,N} \\ Q_{l,N-1} \\ \vdots \\ Q_{l,0} \end{pmatrix}, \quad \bar{b}_l = \begin{pmatrix} 0 \\ 0 \\ \vdots \\ -2ak \sinh Q_{l,N} \\ \vdots \\ 0 \end{pmatrix}, \quad l = 1, 2, \dots, M. \tag{B5}$$

We note that the vector \bar{Q}_l now consists of all the unknowns on the gridline $\phi = \phi_l$ in Fig. 4.

Suppose $\hat{\mathbf{Q}}^T = [\hat{\mathbf{Q}}_1, \hat{\mathbf{Q}}_2, \dots, \hat{\mathbf{Q}}_M]$ is a solution of (B.1). We define a new vector $\tilde{\mathbf{Q}}$ as

$$\tilde{\mathbf{Q}}^T \equiv [\tilde{\mathbf{Q}}_1, \tilde{\mathbf{Q}}_2, \dots, \tilde{\mathbf{Q}}_M], \quad (\text{B6a})$$

$$= [\hat{\mathbf{Q}}_2, \hat{\mathbf{Q}}_3, \dots, \hat{\mathbf{Q}}_M, \hat{\mathbf{Q}}_1]. \quad (\text{B6b})$$

Thus, $\tilde{\mathbf{Q}}$ is obtained by permuting the vectors of $\hat{\mathbf{Q}}$ once; physically this means that $\tilde{\mathbf{Q}}$ differs from $\hat{\mathbf{Q}}$ by the phase factor $\Delta\phi$.

If we substitute $\tilde{\mathbf{Q}}$ into (B1) we find that $\tilde{\mathbf{Q}}$ is also a solution of (B1) because the system of equations

$$\bar{\mathbf{B}}' \cdot \tilde{\mathbf{Q}} = \bar{\mathbf{b}}, \quad (\text{B7})$$

where $\bar{\mathbf{b}}^T = [\bar{\mathbf{b}}_2, \bar{\mathbf{b}}_3, \dots, \bar{\mathbf{b}}_M, \bar{\mathbf{b}}_1]$, is identical to $\bar{\mathbf{B}}' \cdot \hat{\mathbf{Q}} = \bar{\mathbf{b}}$, the only difference being that the equations appear in a different sequence. Similarly, we can continue to cyclically permute the vectors of $\hat{\mathbf{Q}}$ to generate additional solutions with different phases. In general, if there are M grid points in the ϕ direction, we can generate $(M-1)$ different solutions from a known solution, and each solution differs in phase from the known solution by a multiple of the phase factor $\Delta\phi = \lambda/M$.

ACKNOWLEDGMENT

The authors are grateful for the generous support provided by the National Science Foundation under Grant ENG-75-16606. Part of this paper is taken from a Ph.D. dissertation (Liu (1980)) submitted to the Chemical Engineering Department at the Polytechnic Institute of New York.

REFERENCES

1. F. W. DORR, *Soc. Ind. Appl. Math. Rev.* **12** (1970), 248.
2. O. BUNEMAN, A Compact Non-iterative Poisson Solver, Report No. 294, Stanford Univ. Inst. for Plasma Research, 1969.
3. B. L. BUZBEE, G. H. GOLUB, AND C. W. NIELSON, *Soc. Ind. Appl. Math. J. Numer. Anal.* **7** (1970), 627.
4. B. L. BUZBEE, F. W. DORR, J. A. GEORGE, AND G. H. GOLUB, *Soc. Ind. Appl. Math. J. Numer. Anal.* **8** (1971), 722.
5. B. L. BUZBEE AND F. W. DORR, *Soc. Ind. Appl. Math. J. Numer. Anal.* **11** (1974), 753.
6. P. N. SWARZTRAUBER AND R. A. SWEET, *Soc. Ind. Appl. Math. J. Numer. Anal.* **10** (1973), 900.
7. P. N. SWARZTRAUBER, *J. Comput. Phys.* **15** (1974), 46.
8. R. A. SWEET, *Soc. Ind. Appl. Math. J. Numer. Anal.* **11** (1974), 506.
9. R. A. SWEET, *Soc. Ind. Appl. Math. J. Numer. Anal.* **14** (1977), 706.
10. P. N. SWARZTRAUBER, *Soc. Ind. Appl. Math. J. Numer. Anal.* **11** (1974), 1136.
11. P. CONCUS AND G. H. GOLUB, *Soc. Ind. Appl. Math. J. Numer. Anal.* **10** (1973), 1103.
12. B. L. BUZBEE, *Soc. Ind. Appl. Math. J. Numer. Anal.* **14** (1977), 205.
13. R. W. HOCKNEY, in "Methods of Computational Physics" (B. Alder, S. Fernbach, and M. Rotenberg, Eds.), Vol. 9, pp. 135-211, Academic Press, New York, 1969.

14. P. N. SWARZTRAUBER, *Soc. Ind. Appl. Math. Rev.* **19** (1977), 490.
15. R. E. BANK AND P. J. ROSE, *Soc. Ind. Appl. Math. J. Numer. Anal.* **14** (1977), 792.
16. G. D. CRAPPER, *J. Fluid Mech.* **2** (1957), 532.
17. W. KINNERSLEY, *J. Fluid Mech.* **77** (1976), 229.
18. P. F. BYRD AND M. P. FRIEDMAN, "Handbook of Elliptic Integrals for Engineers and Scientists," Springer-Verlag, New York, 1971.
19. M. I. G. BLOOR, *J. Fluid Mech.* **84** (1978), 167.
20. B. CHEN AND P. G. SAFFMAN, *Stud. Appl. Math.* **60** (1979), 183.
21. J. W. ROTTMAN AND D. B. OLFE, *J. Fluid Mech.* **94** (1979), 777.
22. L. W. SCHWARTZ AND J.-M. VANDEN-BROECK, *J. Fluid Mech.* **95** (1979), 119.
23. A. BJÖRCK AND G. H. GOLUB, *Soc. Ind. Appl. Math. Rev.* **19** (1977), 5.
24. T. J. LIU, Ph.D. thesis, Polytechnic Inst. of New York, 1980.
25. C. G. BROYDEN, *Math. Comput.* **19** (1965), 577.
26. R. C. ACKERBERG AND T. J. LIU, "The Effects of Capillarity on the Contraction Coefficient of a Jet Emanating from a Slot," submitted.